In Proceedings of the 36th Annual International Conference of the IEEE Engineering in Medicine and Biology Society

Generalizability of EMG decoding using local field potentials

Agamemnon Krasoulis, *Student Member, IEEE*, Thomas M. Hall, Sethu Vijayakumar,
Andrew Jackson and Kianoush Nazarpour, *Senior Member, IEEE*

***Abstract*— Motor cortical local field potentials (LFPs) have been successfully used to decode both kinematics and kinetics of arm movement. For future clinically viable prostheses, however, brain activity decoders will have to generalize well under a wide spectrum of behavioral conditions. This property has not yet been demonstrated clearly. Here, we provide evidence for the first time, that an LFP-based electromyogram (EMG) decoder can generalize reasonably well across two different types of behavior. We implanted intracortical microelectrode arrays in the primary motor (M1) and ventral pre-motor (PMv) cortices of a rhesus macaque, and recorded LFP and EMG activity from arm and hand muscles of the contralateral forelimb during a two-dimensional (2-D) centre-out isometric wrist torque task (TT), and during free reach and grasp behavior (FB). Selected temporal and spectral features of the LFP signals were used to train EMG decoders using data from both types of behavior separately. We assessed the decoding performance for both within- and across-task cases. The average achieved generalization score was $65 \pm 20\%$, while in many cases individual scores reached 100%.**

I. INTRODUCTION

The ultimate goal of brain-machine interfaces (BMIs) for motor rehabilitation [1] is to enable patients suffering from movement impairment, due to spinal cord injury (SCI), stroke or degenerative disorders [2], [3], to interact with the world physically, for example by controlling robotic interfaces [4], [5], [6], [7], or by restoring partial movement of the native limb through functional electrical stimulation (FES) of muscles [8], [9], [10], [11].

For effective FES, a robust mechanism of decoding muscle activity from cortical signals is required. Traditionally, spiking-activity (SA) of cortical neurons has been used to decode muscle activity recorded subcutaneously by electromyogram (EMG) electrodes [4], [12], [13].

Recently, there has been increasing evidence that motor cortical local field potentials (LFPs) can provide an alternative robust control signal for BMIs for motor rehabilitation. LFP signals have been used on several occasions to decode both kinematics (i.e. hand position and velocity [14], [15], [16], [17]), and kinetics (i.e. EMG activity [18]) of arm movement. LFPs have been found to be informative of movement kinematics even when neuronal SA is not present on the recording electrodes [19]. Evidence about the robustness of LFP signals has been provided by a recent study, which showed that an LFP-based cursor controller exhibited stable performance for a time course of 12 months, during which the decoder was not recalibrated [17].

Although progress in the BMI field has been very rapid during the last two decades, one aspect that has often been neglected is that in real-life prosthetic applications, the decoders of a BMI should generalize well under different behavioral conditions. In this study, we provide evidence that a linear LFP-based EMG decoder is able to generalize reasonably well across two behavioral tasks, including free reach and grasp behavior (FB).

II. METHODS

A. Surgical and electrophysiological procedures

All procedures were carried in accordance with the UK Animals (Scientific Procedures) Act 1986 and approved by the local ethics committee of Newcastle University. We implanted a female rhesus monkey (Macaca mullata) with a 12-channel micro-wire (M/W) and a 32-channel floating microelectrode array (FMA) in the right primary motor cortex (M1), and a 12-channel M/W microelectrode array in the right ventral premotor cortex (PMv). Raw cortical signals were acquired by a digitising 128-channel amplifier at 24.4 kHz. To extract LFP signals, raw data were band-pass filtered between 1 and 300 Hz, and then down-sampled to 977 Hz.

EMG electrodes were implanted subcutaneously in the following 7 forearm and hand muscles of the left forelimb: ECR, ECU, FCR, FCU, FDS, FDP, 1DI (see Table I). The EMG electrodes were routed subcutaneously to a percutaneous connector on the subject's head. Raw EMG signals were analog filtered (10 Hz to 5 kHz bandpass, with a 50 Hz notch filter), and sampled at 12 kHz. For off-line analysis, they were digitally low-pass filtered at 500 Hz, and down-sampled to 2 kHz.

*A. Krasoulis is supported by grants EP/F500385/1 and BB/F529254/1 for the University of Edinburgh School of Informatics Doctoral Training Centre in Neuroinformatics and Computational Neuroscience (www.anc.ac.uk/dtc) from the UK Engineering and Physical Sciences Research Council (EPSRC), UK Biotechnology and Biological Sciences Research Council (BBSRC), and the UK Medical Research Council (MRC). T. Hall is supported by a studentship from the UK MRC. S. Vijayakumar is supported by the Microsoft Research RAEng. Fellowship, EU FP7 Grant TOMSY and [EPSRC EP/H1012338/1]. A. Jackson is a Wellcome Trust Career Development fellow [086561]. The work of K. Nazarpour was supported by the UK MRC [G0802195].

A. Krasoulis is with the Institute for Adaptive and Neural Computation and the Institute of Perception, Action and Behaviour, School of Informatics, University of Edinburgh, Edinburgh, UK A.Krasoulis@sms.ed.ac.uk

T. M. Hall is with the Institute of Neuroscience, Newcastle University, Newcastle, UK t.m.hall@newcastle.ac.uk

S. Vijayakumar is with the Institute of Perception, Action and Behaviour, School of Informatics, University of Edinburgh, Edinburgh, UK sethu.vijayakumar@ed.ac.uk

A. Jackson is with the Institute of Neuroscience, Newcastle University, Newcastle, UK andrew.jackson@newcastle.ac.uk

K. Nazarpour is with the School of Electrical and Electronic Engineering and the Institute of Neuroscience, Newcastle University, Newcastle, UK Kianoush.Nazarpour@newcastle.ac.uk

978-1-4244-7929-0/14/$26.00 ©2014 IEEE

TABLE I

ABBREVIATIONS AND BRIEF FUNCTION DESCRIPTIONS FOR RECORDED MUSCLES

Abbreviation	Full name	Primary function
ECR	Extensor carpi radialis	Extension and radial deviation of the wrist
ECU	Extensor carpi ulnaris	Extension and ulnar deviation of the wrist
FCR	Flexor carpi radialis	Flexion and radial deviation of the wrist
FCU	Flexor carpi ulnaris	Flexion and ulnar deviation of the wrist
FDS	Flexor digitorum superficialis	Flexion of the middle phalanges of the fingers
FDP	Flexor digitorum profundus	Flexion of the fingers
1DI	First dorsal interosseous	Abduction of the index finger

B. Behavioral tasks

We recorded LFP and EMG activity during two different behavioral tasks: a centre-out isometric wrist torque task (TT), and FB. During the TT task, the monkey had to apply a two-dimensional (2-D) isometric left-wrist torque to control the position of a circular cursor on a screen. Each trial began with the cursor in the central 'home' region. Subsequently, a circular target appeared at one of 8 equally-spaced peripheral locations. Following a variable 'cue' period (1.2-2.4 s), the subject had to move the cursor to overlap the target for a fixed 'hold' period (0.6 s). If successful, the subject heard a reward tone and received a fruit reward. During FB, the subject voluntarily reached with its left hand for small pieces of food from a Klüver board. A total number of 10 recording sessions was performed, with each recording session consisting of 50-320 trials of TT followed by 5-15 minutes of FB.

C. Decoding

The following features were extracted from the LFP signals: the local motor potential (LMP), which is the window average of the raw LFP signal [21], [22], and the power in the following five frequency bands: 0-4, 7-20, 70-115, 130-198, 202-300 Hz [17], [18]. The window length for the fast Fourier transform (FFT) calculations was set to 256 points with 207-point overlap, which yielded a new sample every 50.2 ms.

For EMG signals, the temporal envelope was extracted by digital high-pass filtering at 50 Hz (to remove electrocardiogram (ECG) and motion artifacts), full-wave rectification and low-pass filtering at 5 Hz. The processed signals were finally downsampled to 19.5 Hz to match the LFP samples. All filtering was performed both on the forward and backward directions to avoid any phase delays.

For decoding EMG activity from LFP features, we employed the Wiener filter [12]. The length of the linear filters was set to 502 ms. To avoid overfitting the training data, we only used 50 input features to train each individual decoder. The feature selection procedure was performed by using a feature ranking method based on input-output correlations [17], [18].

D. Performance assessment

Training and performance assessment of our EMG decoders was performed using a 5-fold cross-validation (CV) procedure. For each fold, the quality of EMG reconstruction was assessed by using both the coefficient of determination (R^2), and the normalised root-mean-squared-error ($nRMSE$), which consider the correlation and absolute difference between the measured and reconstructed EMG signals, respectively, and are defined as follows:

$$R^2 = \frac{\left(\sum_{j=1}^{M}\left(p_j-\bar{p}\right)\left(\hat{p_j}-\bar{\hat{p}}\right)\right)^2}{\sum_{j=1}^{M}\left(p_j-\bar{p}\right)^2\sum_{j=1}^{M}\left(\hat{p_j}-\bar{\hat{p}}\right)^2}, \tag{1}$$

and

$$nRMSE = \sqrt{\frac{\sum_{j=1}^{M}\left(p_j-\hat{p_j}\right)^2}{n}} \Bigg/ \left(p_{max}-p_{min}\right), \tag{2}$$

where p_j and $\hat{p_j}$ denote measured and reconstructed EMG values for the j^{th} sample of a CV-fold, $\bar{p}$ and $\bar{\hat{p}}$ denote their respective expected values over all the samples of the fold $j = 1, \ldots, M$, and finally, p_{max} and p_{min} denote the maximum and minimum values respectively, of the measured EMG signal within the fold.

To compare within- and across-task decoding performance we used the following two generalization ratios [20]:

$$\mathcal{G}_{R^2}\% = \frac{R^2_A}{R^2_W}, \tag{3}$$

and

$$\mathcal{G}_{nRMSE}\% = \frac{nRMSE_W}{nRMSE_A}, \tag{4}$$

where the W and A indices denote within- and across-task decoding, respectively. Note that, unlike the $nRMSE$ metric, the $\mathcal{G}_{nRMSE}\%$ ratio is defined such that it is an increasing function of the quality of generalization. Folds for which $R^2_W < \theta_W$, where θ_W was defined as the mean R^2_W subtracted by 2.5 times its standard deviation, were discarded from ratios calculations. This elimination procedure was introduced in order to prevent the denominator in Eq. (3) from taking problematically low values. Furthermore, this allowed us to assess the generalization performance of our decoders only for the folds for which within-task performance was reasonably high.

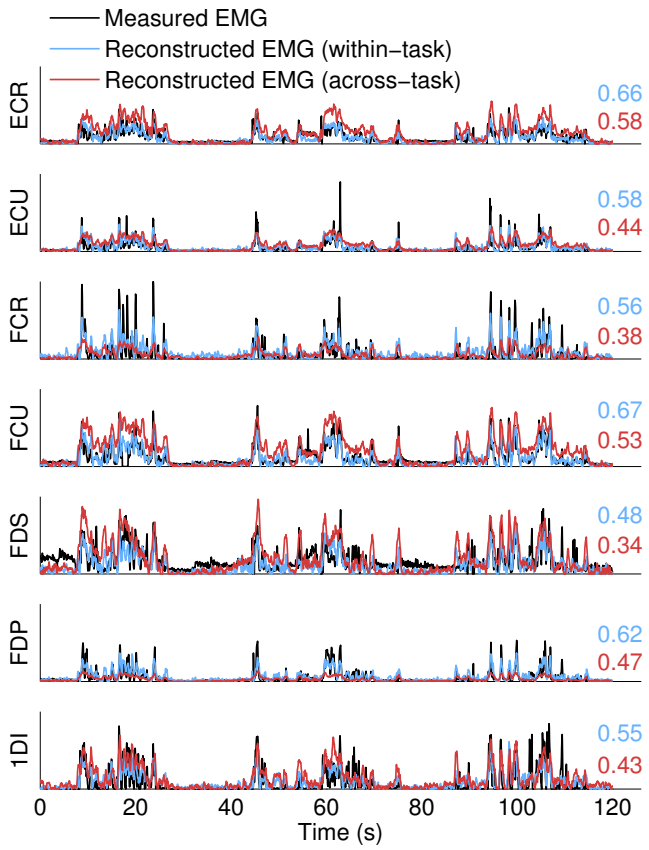

Fig. 1. Example of a typical group of muscle activity from recorded EMG signals (*black line*), along with the within- (*blue line*) and across-task (*red line*) reconstructed signals, during free reach and grasp behavior (FB). Values inset at the top right denote R^2 scores. Overall R^2 scores for this fold (averaged across all muscles) were 0.60 $\pm$ 0.07 and 0.47 $\pm$ 0.10 (mean $\pm$ std), respectively. The corresponding $nRMSE$ scores were 0.09 $\pm$ 0.02 and 0.15 $\pm$ 0.05. For muscle name abbreviations and primary functions, see Table I.

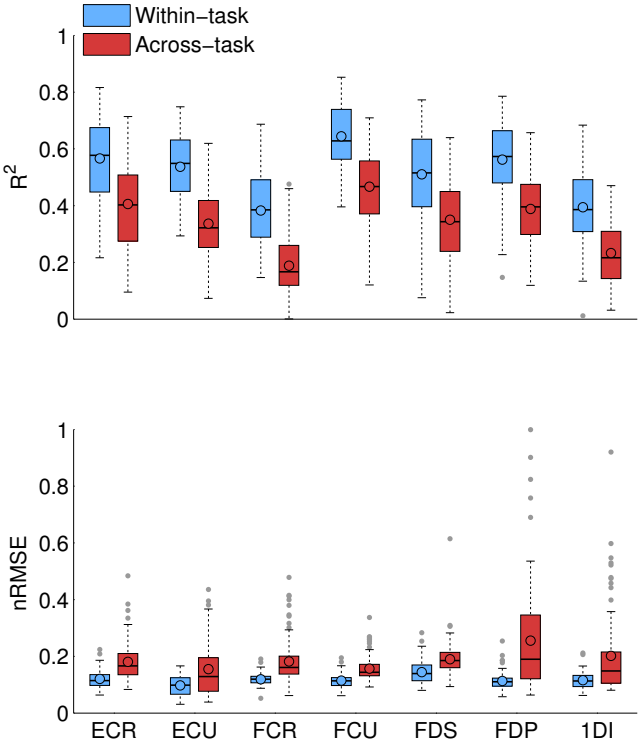

Fig. 2. Summary quartile plots for within- (*blue boxplots*) and across-task (*red boxplots*) decoding performance. Black lines, medians; black circles, means; solid boxes, interquartile ranges; whiskers, overall ranges of nonoutlier data; grey circles indicate outliers. R^2 (*top*), coefficient of determination; $nRMSE$ (*bottom*), normalised root-mean-squared-error. Results averaged across all folds ($n_{folds} = 50$).

III. Results

Traces of recorded EMG activity, along with the reconstructed signals from within- and across-task decoding, are presented in Fig. 1. Values inset at the top right of each panel denote the respective R^2 scores calculated for the shown excerpt, and for each muscle separately.

Fig. 2 summarises the quality of EMG reconstruction for within- and across-task decoding. The overall decoding performance, averaged across all muscles and folds, was R^2 = 0.51 $\pm$ 0.16 and 0.34 $\pm$ 0.16 (mean $\pm$ std, $n = 350$), respectively. The corresponding $nRMSE$ values were 0.12 $\pm$ 0.03 and 0.19 $\pm$ 0.12.

To evaluate the across-task generalizability of our decoders, we computed the $\mathcal{G}_{R^2}\%$ and $\mathcal{G}_{nRMSE}\%$ ratios. The results for each of the recorded muscles are summarised in Fig. 3. The overall generalization performance, averaged across all muscles and folds, was $\mathcal{G}_{R^2}\%$ = 65 $\pm$ 20 and $\mathcal{G}_{nRMSE}\%$ = 73 $\pm$ 23 (mean $\pm$ std, $n = 348$), respectively.

IV. Discussion

Decoding performance slightly degraded in the case of across-task decoding (Fig. 2 and 3). Notably, the $nRMSE$ metric, which represents the generalization error of the decoder, was in some cases very high, even when the correlation between the measured and reconstructed signals was also high. This implies that, although the target signal was successfully tracked, there were scaling and/or offset errors (for instance, see Fig. 1, FDP muscle). The scaling and offset issues were due to the regressors extrapolating to values outside the training data range. In our analyses, we deliberately chose not to make use of the non-linear subsystem of the Wiener cascade filter, which is usually employed for EMG decoding [18], [20], as this would further bias our decoders towards the training task. The scaling and offset errors could potentially be eliminated by fitting a linear or polynomial model to the output of the decoders, similar to the Wiener cascade filter approach, in order to fine-tune the prediction to a specific task. This would only require a very short period of training activity, as the number of fitting parameters would in that case be very small (e.g. 4 parameters for a 3$^{\text{rd}}$-order polynomial).

To the best of our knowledge, this is the first piece of work to demonstrate that muscle activity decoders using LFPs as control signals can generalize over different tasks. Two studies have investigated generalization of EMG reconstruction in the past [20], [23], but both used SA signals from M1 for decoding, while also [20] was limited to investigating decoding performance only across altered conditions within

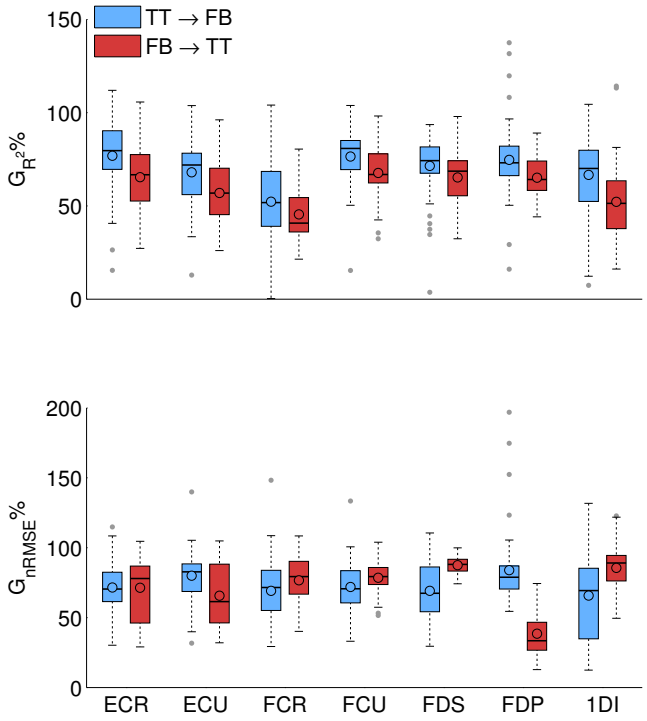

Fig. 3. Summary quartile plots for generalization ratios $\mathcal{G}_{R^2}\%$ (*top*) and $\mathcal{G}_{nRMSE}\%$ (*bottom*). Symbols same as in Fig. 2. Results averaged across all folds ($n_{folds} = 50$).

a fixed behavioral task. A possible limitation of our study might be that it was limited to data coming only from one animal, however, the authors are currently working to extend this work to include data from additional animals.

In conclusion, this study provides evidence for the first time, that a simple linear LFP-based muscle activity decoder can generalize reasonably well across two different types of behavior. The implications of our findings could be of great importance in future design of BMIs for motor rehabilitation, as they provide evidence that motor cortical LFPs might offer a robust control signal for real-life prosthetic applications.

REFERENCES

[1] Homer, M. L., Nurmikko, A. V., Donoghue, J. P., Hochberg, L. R. (2013). Sensors and decoding for intracortical brain computer interfaces. Annual Review of Biomedical Engineering, 15, 383-405.

[2] Hatsopoulos, N. G., Donoghue, J. P. (2009). The science of neural interface systems. Annual Review of Neuroscience, 32, 249-66.

[3] Jackson, A., Zimmermann, J. B. (2012). Neural interfaces for the brain and spinal cord–restoring motor function. Nature Reviews. Neurology, 8(12), 690-9.

[4] Carmena, J. M., Lebedev, M. A., Crist, R. E., O'Doherty, J. E., Santucci, D. M., Dimitrov, D. F., Patil, P. G., Henriquez, C. S., Nicolelis, M. A. L. (2003). Learning to control a brain-machine interface for reaching and grasping by primates. PLoS Biology, 1(2), E42.

[5] Hochberg, L. R., Serruya, M. D., Friehs, G. M., Mukand, J. A, Saleh, M., Caplan, A. H., Branner, A., Chen, D., Penn, R. D., Donoghue, J. P. (2006). Neuronal ensemble control of prosthetic devices by a human with tetraplegia. Nature, 442(7099), 164-71.

[6] Velliste, M., Perel, S., Spalding, M. C., Whitford, A. S., Schwartz, A. B. (2008). Cortical control of a prosthetic arm for self-feeding. Nature, 453(7198), 1098-101.

[7] Collinger, J. L., Wodlinger, B., Downey, J. E., Wang, W., Tyler-Kabara, E. C., Weber, D. J., Schwartz, A. B. (2013). High-performance neuroprosthetic control by an individual with tetraplegia. Lancet, 381(9866), 557-64.

[8] Moritz, C. T., Perlmutter, S. I., Fetz, E. E. (2008). Direct control of paralysed muscles by cortical neurons. Nature, 456(7222), 639-42.

[9] Pohlmeyer, E. A, Oby, E. R., Perreault, E. J., Solla, S. A, Kilgore, K. L., Kirsch, R. F., & Miller, L. E. (2009). Toward the restoration of hand use to a paralyzed monkey: brain-controlled functional electrical stimulation of forearm muscles. PloS One, 4(6), e5924.

[10] Chadwick, E. K., Blana, D., Simeral, J. D., Lambrecht, J., Kim, S. P., Cornwell, A S., Kirsch, R. F. (2011). Continuous neuronal ensemble control of simulated arm reaching by a human with tetraplegia. Journal of Neural Engineering, 8(3), 034003.

[11] Ethier, C., Oby, E. R., Bauman, M. J., Miller, L. E. (2012). Restoration of grasp following paralysis through brain-controlled stimulation of muscles. Nature, 485(7398), 368-71.

[12] Westwick, D. T., Pohlmeyer, E. A, Solla, S. A, Miller, L. E., Perreault, E. J. (2006). Identification of multiple-input systems with highly coupled inputs: application to EMG prediction from multiple intracortical electrodes. Neural Computation, 18(2), 329-55.

[13] Nazarpour, K., Ethier, C., Paninski, L., Rebesco, J. M., Miall, R. C., Miller, L. E. (2012). EMG prediction from motor cortical recordings via a nonnegative point-process filter. IEEE Transactions on Biomedical Engineering, 59(7), 1829-38.

[14] Zhuang, J., Truccolo, W., Vargas-Irwin, C., Donoghue, J. P. (2010). Decoding 3-D reach and grasp kinematics from high-frequency local field potentials in primate primary motor cortex. IEEE Transactions on Biomedical Engineering, 57(7), 1774-84.

[15] Bansal, A. K., Vargas-Irwin, C. E., Truccolo, W., Donoghue, J. P. (2011). Relationships among low-frequency local field potentials, spiking activity, and three-dimensional reach and grasp kinematics in primary motor and ventral premotor cortices. Journal of Neurophysiology, 105(4), 1603-19.

[16] Bansal, A. K., Truccolo, W., Vargas-Irwin, C. E., Donoghue, J. P. (2012). Decoding 3D reach and grasp from hybrid signals in motor and premotor cortices: spikes, multiunit activity, and local field potentials. Journal of Neurophysiology, 107(5), 1337-55.

[17] Flint, R. D., Wright, Z. A, Scheid, M. R., Slutzky, M. W. (2013). Long term, stable brain machine interface performance using local field potentials and multiunit spikes. Journal of Neural Engineering, 10(5), 056005.

[18] Flint, R. D., Ethier, C., Oby, E. R., Miller, L. E., Slutzky, M. W. (2012a). Local field potentials allow accurate decoding of muscle activity. Journal of Neurophysiology, 108(1), 18-24.

[19] Flint, R. D., Lindberg, E. W., Jordan, L. R., Miller, L. E., Slutzky, M. W. (2012b). Accurate decoding of reaching movements from field potentials in the absence of spikes. Journal of Neural Engineering, 9(4), 046006.

[20] Cherian, A., Krucoff, M., Miller, L. E. (2011). Motor cortical prediction of EMG: evidence that a kinetic brain-machine interface may be robust across altered movement dynamics. Journal of Neurophysiology, 564-575.

[21] Mehring, C., Nawrot, M. P., de Oliveira, S. C., Vaadia, E., Schulze-Bonhage, A., Aertsen, A., Ball, T. (2005). Comparing information about arm movement direction in single channels of local and epicortical field potentials from monkey and human motor cortex. Journal of Physiology, 98(4-6), 498-506.

[22] Schalk, G., Kubnek, J., Miller, K. J., Anderson, N. R., Leuthardt, E. C., Ojemann, J. G., Limbrick, D., Moran, D., Gerhardt, L. A., Wolpaw, J. R. (2007). Decoding two-dimensional movement trajectories using electrocorticographic signals in humans. Journal of Neural Engineering, 4(3), 264-75.

[23] Pohlmeyer, E. A., Solla, S. A., Perreault, E. J., Miller, L. E. (2007). Prediction of upper limb muscle activity from motor cortical discharge during reaching. Journal of Neural Engineering, 4(4), 369-79.